Incorporating External constraints to MicroBooNE/SBN Oscillation Searches

REU Program at Columbia University - Nevis Labs

Sarah Heller¹

¹Montana State University

August 2, 2024

Abstract

MicroBooNE is one of the current leading experiments in the search for neutrino oscillations. As such, it is important to characterize the experiment's sensitivity to different sterile neutrino oscillation models and compare/constrain the sensitivity with external experimental results. This study performs a χ^2 sensitivity analysis on simulated MicroBooNE Wire-Cell events according to the 3+1 sterile neutrino model, using simultaneous ν_e appearance, ν_e disappearance, and ν_μ disappearance channels. The sensitivity regions are then further constrained using best-fit parameters from the Ice-Cube experiment ($\Delta m_{41}^2 = 4.5 eV$ and $\sin^2(2\theta_{24}) = 0.1$) and the upper parameter limit set by PROSPECT ($\sin^2(2\theta_{14}) \gtrsim 0.02$). When considering both of these external constraints, MicroBooNE loses sensitivity to the globally allowed parameter region for the 3+1 sterile neutrino model.









Contents

1	Background			3
	1.1 Neutrinos			3
	1.2 MicroBooNE			4
	1.3 3+1 Oscillations			5
	Introduction to Neutrino Mixing			5
	Oscillation Probability Equations			6
	Appearance vs Disappearance			8
2	Sensitivity Analysis Motivation			8
3	Methods			9
	3.1 MC Sample Events			9
	3.2 Plotting ν_e and ν_μ Spectra			10
	3.3 χ^2 Analysis			12
	Why chi2			12
	Equations			12
	Short Example			13
	Applying to Oscillations			15
4	Results			16
	4.1 χ^2 Contours in MicroBooNE Parameter Space			16
	4.2 Incorporating External Constraints			19
5	Conclusion			21
A	Acknowledgements			21
References				22

 $Email\ Correspondence:\ shellers tudent@gmail.com$

All python Jupyter Notebook code used in this study can be found on my GitHub at

https://github.com/SarahPyth/Nevis_Labs_Neutrino_Reu_2024

All MC simulation data was provided by FermiLab and require FermiLab permission to access

1 Background

1.1 Neutrinos

Neutrinos are one type of fundamental particle predicted by the Standard Model of particle physics. This Standard Model (SM) is the mathematical framework by which scientists understand the building blocks of matter (particles) and the glue that hold them together (forces).

There are two main sub-classes of particles: leptons and quarks. Quarks are spin 1/2 particles with electrical charge -1/3 or 2/3 that combine to create other particles, such as protons and neutrons (3 quarks).

Then, there are leptons, which are spin 1/2 with electrical charge of -1 or 0, but do not combine to form new particles. Within leptons are the electron, muon, and tau, along with their cousins the neutrinos.

Standard Model of Elementary Particles three generations of matter

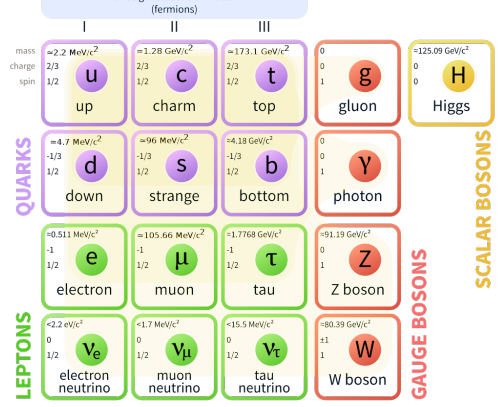


Figure 1: Outline of the Standard Model including quarks, leptons, and force carriers

The three forces in the SM are the weak force, which acts on both quarks and leptons, the strong force, which only acts on quarks, and the electromagnetic force, which only acts on electrically charged particles.

Looking more closely at neutrinos, there are 3 flavours that mirror their cousins: the electron neutrino (ν_e), the muon neutrino (ν_{μ}), and the tau neutrino (ν_{τ}). Additionally, neutrinos have a charge of 0, meaning they don't interact with the electromagnitic force, and as neutrinos are leptons, they also don't interact with the strong force. Thus, neutrinos can only interact with the weak force.

So why should we still care about and study neutrinos if they are understood by the Standard Model? Well, it turns out there are still physical phenomena that are not predicted by the SM, implying the model has small inaccuracies or is incomplete. One such phenomenon is the mass of neutrinos. Traditionally, the SM predicted that neutrinos were massless. However, experimental evidence has since proved that neutrinos DO have mass, though it's several orders of magnitude smaller than any other known particle.

This revelation on neutrino mass started in the late 1900s, when physicists were noticing several experimental neutrino anomalies. When measuring the flux of solar ν_e produced by the sun, detectors were counting only about a third of the predicted number. Additionally, when measuring the flux of atmospheric neutrinos, there was a deficit in the ν_{μ}/ν_{e} flux ratio compared to the predicted model [1].

Further study into these anomalies showed that the deficits of different neutrino flavors were proportional to each other and could be explained by the neutrinos switching, or "oscillating", between flavours as they travel. This oscillation phenomenon occurs because of the separation between neutrino mass eigenstates and flavour eigenstates, which will be further explained in Sec. 1.3.

Thus, the presence of neutrino oscillations directly implies a mass difference between different flavours, meaning neutrinos cannot have the 0 mass the SM originally predicted. As neutrinos cannot receive their mass through the same Higgs mechanism as other particles (since this would have been included in the SM), neutrino oscillations offer a tantalizing glimpse into physics beyond the standard model for physicists to explore.

1.2 MicroBooNE

After the detection of solar and atmospheric neutrino oscillations, neutrino experiments moved onto Earth through the use of particle accelerators and detectors. One of these early accelerator experiments was the Liquid Scintillator Neutrino Detector (LSND) at Los Alamos National Lab. In addition to the different neutrino source, LSND also looked at neutrinos that had traveled a much shorter distance, or baseline, before being detected.

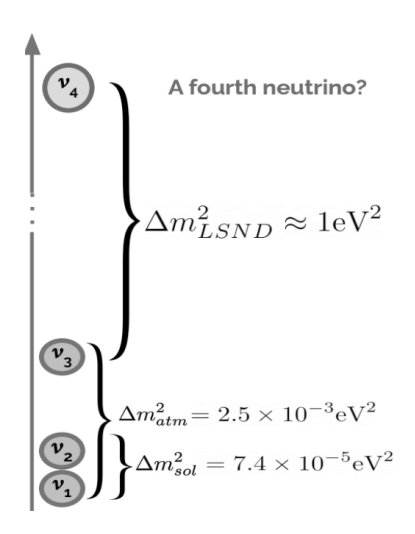


Figure 2: Differences in neutrino mass eigenstates and their corresponding oscillation baselines, with the theoretical 4th sterile neutrino having a much larger mass difference compared to the 3 known neutrinos

At the time, short-baseline neutrino oscillations were not expected as the mass differences between the 3 known neutrino eigenstates corresponded to the previously seen long-baseline oscillations (solar and atmospheric distances) as seen in Fig. 2. Thus, when LSND measured an excess of ν_e , the theoretical model of neutrinos was forced to expand again. One of the leading theories for short-baseline oscillations is the "sterile neutrino", a theoretical 4th type of neutrino that lacks any flavour or interaction with the weak force. This sterile neutrino, if it had a much higher or lower mass, might create the required mass difference to facilitate oscillations with other neutrino flavours at such short distances.

The MiniBooNE experiment at FermiLab was created to further investigate these short-baseline oscillations, and then found an even more anomalous ν_e excess at low energies (called the Low Energy Excess or LEE). Thus, MicroBooNE was created to replace MiniBooNE and probe for these possible signals of low energy short-baseline oscillations.

The MicroBooNE experiment consists of a Liquid Argon Time Projection Chamber detector (LArTPC) and Booster neutrino beamline located at FermiLab. As shown in Fig. 3, the process starts with protons being accelerated, then shot towards the detector through several layers: empty space (where the protons can decay into particle showers, producing neutrinos), absorber (where any non-neutrino particles are stopped), and dirt (where neutrinos can travel uninhibited and experience short-baseline oscillations). Finally, the neutrinos reach the LArTPC detector, which measures the flux (or number) of neutrinos and their flavour. This is achieved using dense argon gas to increase the chance of a neutrino-molecule interaction within the detector and then by measuring the electrical current caused by charged particles released in the interaction. The LArTPC can also distinguish between the neutrino flavours (as well as sort out other background

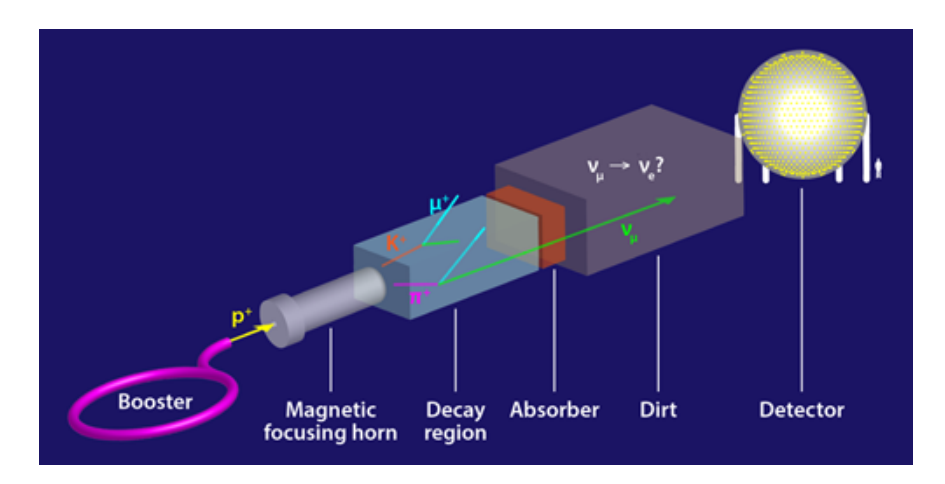


Figure 3: MicroBooNE experiment diagram, starting with neutrino beam from accelerator and ending at LArTPC detector. Image Credit: APS/Alan Stonebraker

particles) based on the specific interaction characteristics, such as total energy, shape, size of particle tracks, and others.

MicroBooNE's neutrino beam is 99% ν_{μ} and $\bar{\nu}_{\mu}$ (muon antineutrinos) and <1% ν_{e} , with an average energy of 0.5 GeV. The entire length of the experiment, from beam production to detector, is 470 meters [2]. These energy and distance specifications were chosen to optimize the predicted neutrino oscillation probabilities (read more in Sec. 1.3) based on previous experiments' best fits for parameters.

1.3 3+1 Oscillations

In this study, I focus on examining the 3+1 sterile neutrino model, which assumes there are the three normal neutrinos (ν_e , ν_μ , ν_τ) and one additional sterile neutrino (ν_s). This is the minimal model with the addition of only a single sterile neutrino in comparison to other models such as the 3+2 or 3+3. However, no sterile neutrino model has been completely ruled out yet, so I chose to focus on this simplest case.

Introduction to Neutrino Mixing

To start explaining the mechanism behind 3+1 neutrino oscillations, lets take one step back and first consider the known 3 neutrino model. In this model, the 3 neutrinos ν_e , ν_μ , and ν_τ are all in definitive flavour states, meaning they are allowed to interact with the weak force as an electron, muon, or tau neutrino. However, it turns out that we cannot define a specific mass to each of these flavour-state neutrinos. This is dissimilar to most other particles, where one can look up the exact mass for a known particle. Instead, for the neutrinos, each ν_e , ν_μ , ν_τ is actually a linear combination of different mass eigenstates, which we call ν_1 , ν_2 , and ν_3 .

Conversely, this means we can also consider each neutrino mass eigenstate ν_1 , ν_2 , ν_3 to actually be a linear combination of *flavour eigenstates*. In Fig. 4 below, this mixing of mass-states and flavour-states is shown as the different color components (which correspond to

flavour eigenstates) making up each mass eigenstate. For example, ν_1 is consists of mostly ν_e in combination with smaller fractions of ν_μ and ν_τ .

When a neutrino is freely traveling through space, it is in one of the mass eigenstates and does have a definite mass. But then, when it interacts with another particle through the weak force, the neutrino snaps into one of its possible flavour eigenstates, as the weak force only impacts the flavour-states and not the mass-states. Thus, traveling neutrinos can't be defined as a ν_e , ν_μ , or ν_τ until they interact and are forced to "choose" which neutrino flavour they will be for the weak force interaction. This "choosing" is actually done probabilistically with each mass-state neutrino having a different probability of swapping into each flavour-state according to their specific combination (this can be seen as the differing color combinations for each mass-state in Fig. 4). So, as a neutrino travels, it can actually change it's flavour-state between 2 different interactions (or measurements) and look like it is swapping between flavours. This phenomenon is called neutrino oscillation.

For the 3+1 model, there is an additional sterile neutrino ν_s included in this mass mixing, meaning there is also an additional ν_4 mass eigenstate. This addition of a sterile flavour-state means that sometimes when a neutrino enters an interaction and becomes a specific flavour, it might become "sterile" and then continue on without actually interacting with the weak force at all. This means that the sterile neutrino state cannot be directly detected and can only be inferred through the oscillation of other neutrino flavours into or from sterile neutrinos in experiments.

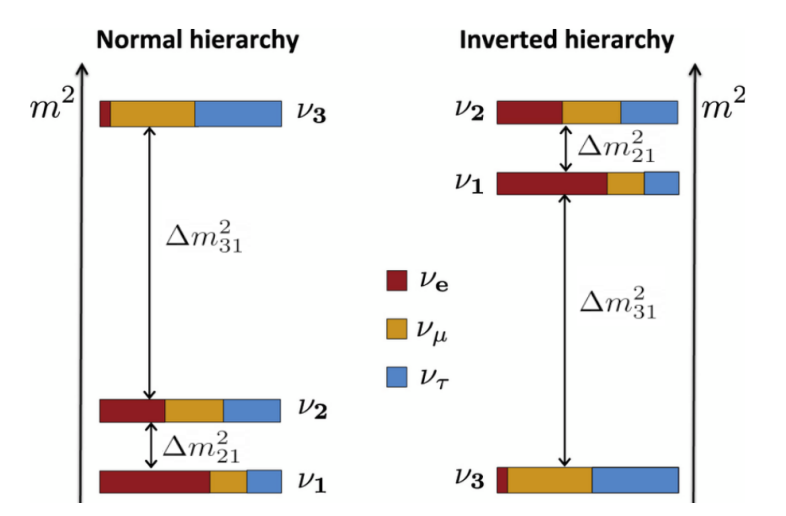


Figure 4: Linear combination of neutrino mass eigenstates and flavour eigenstates for the three neutrino model. The mass hierarchy, or the ordering of the ν_1 , ν_2 , and ν_3 mass eigenstates from lightest to heaviest, is unknown as only the mass differences can be measured through oscillations. This means the normal hierarchy and the inverted hierarchy shown here are equally as likely to be true. Image Credit: Adrián-Martínez et al (2016) [3]

Oscillation Probability Equations

Mathematically, we can express the mixing of neutrino mass eigenstates and flavour eigenstates as a matrix rotation between the 2 sets:

$$\begin{pmatrix}
\nu_{e} \\
\nu_{\mu} \\
\nu_{\tau} \\
\nu_{s}
\end{pmatrix} = \begin{pmatrix}
U_{e1} & U_{e2} & U_{e3} & U_{e4} \\
U_{\mu 1} & U_{\mu 2} & U_{\mu 3} & U_{\mu 4} \\
U_{\tau 1} & U_{\tau 2} & U_{\tau 3} & U_{\tau 4} \\
U_{s1} & U_{s2} & U_{s3} & U_{s4}
\end{pmatrix} \begin{pmatrix}
\nu_{1} \\
\nu_{2} \\
\nu_{3} \\
\nu_{4}
\end{pmatrix} \tag{1}$$

From this matrix rotation, we can calculate the probabilities of each flavour-state either remaining the same flavour or swapping to a different flavour between 2 measurements (based on the different amounts of each flavour in the mass-state linear combination, represented as the U's in Eq. 1). For this study, the relevant probability equations are:

$$P_{\nu_e \to \nu_e} = 1 - \sin^2(2\theta_{ee})\sin^2(1.27\Delta m_{41}^2 L/E)$$
 (2)

$$P_{\nu_{\mu}\to\nu_{\mu}} = 1 - \sin^2(2\theta_{\mu\mu})\sin^2(1.27\Delta m_{41}^2 L/E)$$
(3)

$$P_{\nu_{\mu}\to\nu_{e}} = \sin^{2}(2\theta_{\mu e})\sin^{2}(1.27\Delta m_{41}^{2}L/E) \tag{4}$$

Equations 2 and 3 refer to the probability of an electron or muon neutrino remaining the same flavour after a certain distance traveled (called the survival probability). Equation 4 refers to the probability of an electron neutrino swapping to a muon neutrino (or vice-versa) after a certain distance (called the appearance probability).

There are six unknown parameters in these oscillation probability equations, and they are defined as [4]:

• θ_{ee} = This is the flavour mixing angle between two electron neutrinos and characterizes their mass-state mixing proportions. In relation to the mixing matrix in Eq. 1 or mass mixing angles:

$$\sin^2(2\theta_{ee}) = 4(1 - |U_{e4}|^2)|U_{e4}|^2 \approx \sin^2(2\theta_{14})$$
(5)

• $\theta_{\mu\mu}$ = This is the flavour mixing angle between two muon neutrinos and characterizes their mass-state mixing proportions. In relation to the mixing matrix in Eq. 1 or mass mixing angles:

$$\sin^2(2\theta_{uu}) = 4(1 - |U_{u4}|^2)|U_{u4}|^2 \approx \sin^2(2\theta_{24}) \tag{6}$$

• $\theta_{\mu e}$ = This is the flavour mixing angle between an electron and muon neutrino, charaterizing their mass-state mixing proportions. In relation to the mixing matrix in Eq. 1 or mass mixing angles:

$$\sin^2(2\theta_{\mu e}) = 4|U_{e4}|^2|U_{\mu 4}|^2 \approx \frac{1}{4}\sin^2(2\theta_{14})\sin^2(2\theta_{24}) \tag{7}$$

• Δm_{41}^2 = The difference in squared masses between the ν_1 and ν_4 mass eigenstates,

$$\Delta m_{41}^2 = m_4^2 - m_1^2$$

- L = The distance between two measurement points in meters, also called the baseline
- E = The energy of the neutrino in GeV
- 1.27 = This is a constant that adjusts for the given units of meters and GeVs

Appearance vs Disappearance

When physicists take experimental measurements of neutrinos, we can only measure the total flux of ν_e and/or ν_{μ} at a specific moment. Thus, in order to measure neutrino oscillations, we compare the flux measurements of ν_e and ν_{μ} at the start of the neutrino beam to the flux measurements at the detector.

In this study, since I'm using MicroBooNE simulation data (read more in Fig. 3.1), the only oscillations that are predicted to occur by the 3+1 model are the short-baseline oscillations with the sterile neutrino ($\nu_e \to \nu_s, \nu_\mu \to \nu_s, \nu_s \to \nu_e, \nu_s \to \nu_\mu$).

Thus, we expect some of the ν_e and ν_μ that were originally in the beam (called the intrinsic ν_e and ν_μ) to "disappear" as they oscillate to a sterile ν_s that we can't measure or observe. This means there would be less neutrinos counted at the detector than there were at the start of the neutrino beam,

However, within the space between the accelerator and the detector, some neutrinos might oscillate to sterile and then back again to a detectable flavour. This means the multi-step oscillation $\nu_{\mu} \to \nu_{s} \to \nu_{e}$ can essentially look like a direct short-baseline $\nu_{\mu} \to \nu_{e}$ oscillation, which could only be allowed at such short distances by transitioning through the sterile-state.

Since the original MicroBooNE neutrino beam is composed primarily of ν_{μ} (with only <1% ν_{e}), this multi-step sterile oscillation would occur more frequently as $\nu_{\mu} \rightarrow \nu_{e}$ than in the other direction. Thus, we would then expect to see more ν_{e} "appear" at the detector than there were originally in the beam as some of the ν_{μ} oscillate into ν_{e} via the sterile-state.

Throughout the last few decades, different neutrino experiments have focused primarily on appearance and/or disappearance searches based on which flavours of neutrinos they could detect. For example, LSND was an appearance search in that the detector could only measure ν_e and so the analysis focused on finding and excess number of ν_e over the background noise. Since MicroBooNE has the capability of deetecting both ν_e and ν_μ , this study combines the appearance of ν_e and the disappearance of ν_μ methods in order to maximize the amount of information available to the analysis.

2 Sensitivity Analysis Motivation

Sensitivity studies are an important part of the experimental process because physicists need a way to quantify how sensitive an individual experiment's measurements will be (how small or precise) in a way that can be compared to other experiments. In particular, we also need to determine how sensitive an experiment is to specific models.

To understand this, first consider the overall goal of a neutrino oscillation experiment: to take flux data and fit different oscillation probability models to the observations in order to find the best parameters (θ_{ee} , $U_{\mu4}$, Δm_{41}^2 , etc.) that explain the observations. However, some parameter combinations will only cause very small observable oscillation effects due to the low frequency or amplitude of their oscillations. This means that if an experiment is unable to detect those very small effects, we might not be able to identify that an oscillation is actually occurring.

Since MicroBooNE cannot detect every small variation in flux, due to the inherent uncertainty in distinguishing between background "noise" and true oscillation "signal", it is

important to determine which parameter regions MicroBooNE is sensitive to. These regions will be where we can statistically differentiate between the background neutrinos and the predicted oscillation neutrinos.

Overall, a sensitivity study looks at all possible predictions of what the MicroBooNE detector would measure based on different parameter combinations, and then compares these predicted signals to the known background to determine which parameter combinations the experiment could possibly detect if that combination contained the "true" parameters. Thus, if the true parameters fall outside of the sensitive region, MicroBooNE would be unable to detect them and could rule out all parameter combinations within it's sensitivity region.

In this study, I will be performing a sensitive analysis for the MicroBooNE experiment considering the 3+1 sterile neutrino model with parameters U_{e4} , $U_{\mu4}$, and Δm_{41}^2 . This analysis is different from previous MicroBooNE sensitivity studies [5] in that it includes the predictions for ν_e appearance, ν_e disappearance, and ν_{μ} disappearance combined, in comparison to only considering the appearance or disappearance channel. Additionally, I will be incorporating several external best-fit parameters and parameter limits into the analysis using previous results from the IceCube and PROSPECT experiments.

3 Methods

3.1 MC Sample Events

When performing a sensitivity study, it can be helpful to use Monte Carlo (MC) simulation data instead of real events. This is because the MC sample includes "truth-level" information on all neutrino events in addition to the reconstructed values. When looking at actual science run data, physicists only have access to the neutrinos variable values (such as energy, flavour type, neutrino baseline, etc.) that we can reconstruct from the raw detector information.

However, in a MC simulation, all aspects of the MicroBooNE experiment (including the neutrino beam and detector) are digitally re-created in a simulation software. Then, the software can use these system specifications and probability models to simulate an entire detection run: what the neutrino beam exactly consists of, which interactions happen, which neutrinos oscillate, what the detector would receive, and what the reconstruction software would read out.

The important part of the simulation process is that all of the information prior to the reconstruction stage, which is unknown during a physical run, is saved and viewable to researchers. We call these the "truth-level" values as they include the true energy (and flavour type, neutrino baseline, etc.) of each neutrino the simulation produced before it interacts with the detector and reconstruction software.

This is helpful for sensitivity studies because we can know the exact intrinsic ν_e and ν_{μ} flux in the neutrino beam before oscillations, and then accurately compare this to the flux signal measured by the detector after oscillations.

In this study, I utilized a Monte Carlo Simulation Sample from the Wire-Cell reconstruction software. In particular, I used the following FermiLab files as my MC events:

- The charged-current (CC) channel from the "NumuSelection_Modern_Uboone_Lite" file as my intrinsic ν_{μ} events
- The "NueSelection_Modern_UBOONE_Intrinsic_Nue_Lite" file as my intrinsic ν_e events
- The "NueSelection_Modern_UBOONE_Nu_Osc_Lite" file as my fully oscillated ν_{μ} events (assuming a $\nu_{\mu} \rightarrow \nu_{e}$ probability of 100%) after accounting for detector cross-section, flux, and detection uncertainties

3.2 Plotting ν_e and ν_μ Spectra

The way we visualize the flux measurements from the MicroBooNE detector is by using neutrino energy histograms. This allows us to count the total number of measured neutrino events and categorize them into bins based on their neutrino energy values. When representing these flux counts, we want to choose large enough bin widths so each individual bin has >5 events(so we have statistical power), but small enough bin widths that we can see the finer distinctions between different energy levels (not just lumping all the events into a few bins).

In the case for the MicroBooNE MC sample, I chose to use variable bin widths in order to accomplish both of these goals. Since there are very few high energy events, I grouped together several smaller bins into one larger bin to increase the bin count number, while leaving the bin width smaller at lower energies where there are more events.

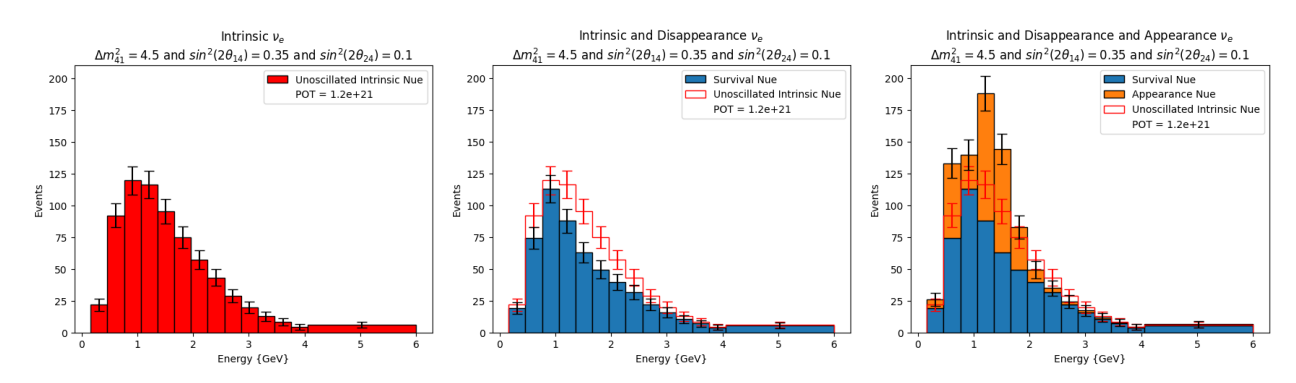


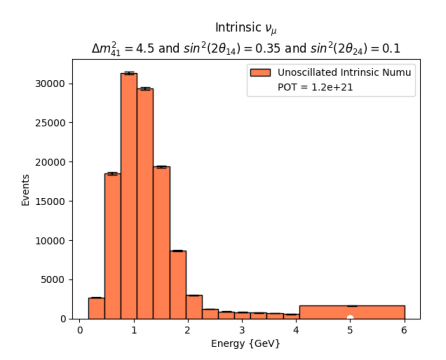
Figure 5: Layered ν_e Spectra, from the intrinsic ν_e flux, to the survival ν_e flux, to the survival ν_e flux

To further understand the appearance and disappearance mechanisms of neutrino oscillation, I plotted a step-by-step layering of the electron neutrino ν_e spectra using the MC truth-level values, as shown in Fig. 5. Each of these layers was normalized to a Proton on Target (POT) value of 1.2e21, essentially normalizing the number of events based on how many initial protons were used in the simulation accelerator. Since these histogram bins represent a counting process, they also have an inherent statistical error in them that is equal to the \sqrt{N} for each bin, represented by vertical error bars.

• Layer 1 (red bars in Fig. 5) = The intrinsic ν_e in the neutrino beam as the beam leaves the accelerator (the background ν_e)

- Layer 2 (blue bars in Fig. 5) = The survival ν_e in the neutrino beam as the beam hits the detector. These counts are calculated by applying the $P_{\nu_e \to \nu_e}$ probability equation to each individual intrinsic ν_e as a weight, predicting how many of the initial ν_e will remain ν_e
- Layer 3 (orange bars in Fig. 5) = The appearance ν_e in the neutrino beam as the beam hits the detector. These counts are calculated by taking the fully unoscillated ν_{μ} events and applying the $P_{\nu_{\mu} \to \nu_{e}}$ probability equation to each individual intrinsic ν_{μ} , predicting how many ν_{μ} will oscillate into a ν_{e} and be measured by the detector

Then, we compare the total ν_e that is measured at the detector (survival ν_e + appearance ν_e) to the original intrinsic ν_e flux to determine how the number of electron neutrinos in the beam has changed due to oscillations. As the detector cannot differentiate between which ν_e are "survival" or "appearance" neutrinos, we can only measure their combined flux and thus can have some degeneracy between the number of ν_e that disappeared vs appeared within the neutrino beam (this degenergy is explored more in [6] and [7])



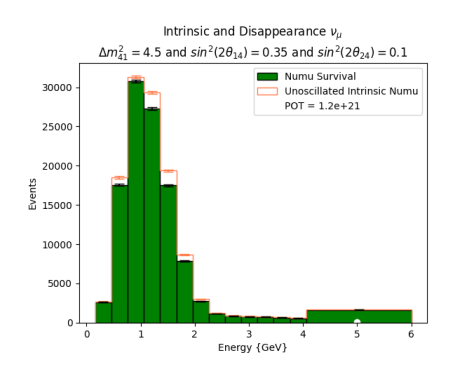


Figure 6: Layered ν_{μ} Spectra, from the intrinsic ν_{μ} flux to the survival ν_{μ} flux

To help counter this degeneracy, I also plotted the muon neutrino ν_{μ} spectra considering ν_{μ} disappearance in Fig. 6. Here we only have two layers as I don't consider ν_{μ} appearance (this is because the expected count is very small due to the <1% of ν_{e} originally in the beam).

- Layer 1 (orange bars on Fig. 6) = The intrinsic ν_{μ} in the neutrino beam as the beam leaves the accelerator
- Layer 2 (green bars on Fig. 6) = The survival ν_{μ} in the neutrino beam as the beam hits the detector. These counts are calculated by applying the $P_{\nu_{\mu} \to \nu_{\mu}}$ probability equation to each individual intrinsic ν_{μ} , predicting how many of the initial ν_{μ} will remain ν_{μ}

Figures 5 and 6 contain the spectra for the specific combination of oscillation parameters $\Delta m_{41}^2 = 4.5 eV$, $sin^2(2\theta_{14}) = 0.35$, and $sin^2(2\theta_{24}) = 0.1$. For this sensitivity study, I constructed the ν_e and ν_μ spectra for 2,700 parameter combinations, each with a different Δm_{41}^2 , U_{e4} , and $U_{\mu 4}$.

3.3 χ^2 Analysis

Why χ^2 ?

From a statistical point of view, there is always some uncertainty to measurements and models, so we need a way to determine if differences between the expected model and observed data come from underlying physics, or if they are just random fluctuations in the measurements. If the difference between prediction and observation is large, the model is likely not accurate and the predictions are incorrect. Whereas, if the difference is small, the differences might just come from inherent measurement noise and the prediction can be considered a good fit. The χ^2 test was developed by statisticians to help quantify this difference and determine if a prediction is a good fit for the observed data or not.

Since we need to quantify the difference between the oscillation signal and the background intrinsic flux on the ν_e and ν_μ spectra for each oscillation parameter combination, the χ^2 test is a good statistical technique to use. This will then allow us to determine which regions of the parameter space the MicroBooNE experiment is sensitive too (where the signal can statistically be differentiated from the background neutrinos).

In order to define a cut-off value between a prediction fitting an observation and NOT fitting an observation, we use χ^2 critical values. These values are determined using statistical models and each correlate to a specific confidence level (CL) that we then have in that given model prediction. These critical values thus depend on how much confidence a physicist requires to have in their prediction and how many free parameters are being simultaneously fit in that prediction (called degrees of freedom, or dof).

For example, with a prediction model that contains three parameters (dof = 3), the critical value $\chi^2 = 6.251$ corresponds to the confidence level of 90%. If the χ^2 calculation for the observed data and the model produces a $\chi^2 > 6.251$, then we can be 90% confident that the model does NOT fit the data. On the other hand, if the $\chi^2 < 6.251$, we cannot be sure if any observed differences come from a true difference between the model and observed data, or if they come from statistical noise, so we can only say we are 90% confident the model IS a good fit to the data.

In either case ($\chi^2 > CriticalValue$ or $\chi^2 < CritialValue$), we cannot be 100% certain in our conclusion as the natural statistical fluctuations could just be abnormally large or small. However, the larger the χ^2 value gets, the more confident we can be that the model is incorrect, and the smaller the χ^2 value gets, the more confident we can be that the model is correct.

χ^2 Equation

The generic χ^2 equation that takes into account correlation between bin counts and systematic errors can be written in summation form as [8]:

$$\chi^2 = \sum_{i}^{N} \sum_{j}^{N} (Observe_i - Expect_i) * M_{ij}^{-1} * (Observe_j - Expect_j)$$
 (8)

Where M is the full covariance matrix encapsulating the expected data's following errors added in quadrature (with ρ_{ij} being the correlation coefficient between bins i and j) [9]:

- σ_{stat}^2 statistical error = N_i
- σ_{flux}^2 systematic flux error = $N_i * N_j * \sigma_{flux,i} * \sigma_{flux,j} * \rho_{flux,ij}$
- σ_{cross}^2 systematic cross-section error = $N_i * N_j * \sigma_{cross,i} * \sigma_{cross,j} * \rho_{cross,ij}$
- σ_{detect}^2 systematic detection error = $N_i * N_j * \sigma_{detect,i} * \sigma_{detect,j} * \rho_{detect,ij}$

Thus, each diagonal M_{ii} element with $\rho_{ii} = 1$ can be calculated as:

$$M_{ii} = \sigma_{stat,i}^2 + \sigma_{flux,i}^2 + \sigma_{cross,i}^2 + \sigma_{detect,i}^2$$
(9)

And each off-diagonal M_{ij} element can be calculated as:

$$M_{ij} = \sigma_{flux,ij}^2 + \sigma_{cross,ij}^2 + \sigma_{detect,ij}^2 \tag{10}$$

3 Bin Example

To fully understand the χ^2 calculation, I will present the step-by-step calculation for a simple histogram containing only three bins. Let us consider the following expected/predicted and observed bin counts:

$$Data_{expected} = \begin{bmatrix} 10 & 2 & 6 \end{bmatrix}$$
$$Data_{observed} = \begin{bmatrix} 20 & 3 & 8 \end{bmatrix}$$

And the following average systematic uncertainties and bin correlations found from previous MicroBooNE simulation studies:

$$Flux_{Systematics}: \sigma_{flux,i} = 0.15, \rho_{flux,ij} = 0.5$$

$$Cross - Section_{Systematics}: \sigma_{cross,i} = 0.2, \rho_{cross,ij} = 1$$

$$Detection_{Systematics}: \sigma_{detect,i} = 0.03, \rho_{detect,ij} = 0$$

Then, the full covariance matrix M will be the linear combination of the four following matrices:

• The statistical error matrix M_{stat} , with elements $\sigma_{stat,i}^2 = N_{i,expect}$

$$M_{stat} = \left[\begin{array}{ccc} 10 & 0 & 0 \\ 0 & 2 & 0 \\ 0 & 0 & 6 \end{array} \right]$$

• The Flux systematic error M_{flux} , with elements $\sigma_{flux,ij}^2 = N_{i,expect} * N_{j,expect} * \sigma_{flux,i} * \sigma_{flux,ij} * \rho_{flux,ij}$

$$M_{flux} = \begin{bmatrix} 10*10*0.15*0.15*1 & 2*10*0.15*0.5 & 6*10*0.15*0.15*0.5 \\ 10*2*0.15*0.15*0.5 & 2*2*0.15*0.15*1 & 6*2*0.15*0.15*0.5 \\ 10*6*0.15*0.15*0.5 & 2*6*0.15*0.15*0.5 & 6*6*0.15*0.15*1 \end{bmatrix}$$

$$= \begin{bmatrix} 2.25 & 0.225 & 0.675 \\ 0.225 & 0.09 & 0.135 \\ 0.675 & 0.135 & 0.81 \end{bmatrix}$$

• The Cross-section systematic error $M_{cross,ij}$, with elements $\sigma_{cross,ij}^2 = N_{i,expect} * N_{j,expect} * \sigma_{cross,i} * \sigma_{cross,ij} * \rho_{cross,ij}$

$$M_{cross} = \begin{bmatrix} 10*10*0.2*0.2*1 & 2*10*0.2*0.2*1 & 6*10*0.2*0.2*1 \\ 10*2*0.2*0.2*1 & 2*2*0.2*0.2*1 & 6*2*0.2*0.2*1 \\ 10*6*0.2*0.2*1 & 2*6*0.2*0.2*1 & 6*6*0.2*0.2*1 \end{bmatrix} = \begin{bmatrix} 4 & 0.8 & 2.4 \\ 0.8 & 0.16 & 0.48 \\ 2.4 & 0.48 & 1.44 \end{bmatrix}$$

• The Detection systematic error M_{detect} , with elements $\sigma_{detect,ij}^2 = N_{i,expect} * N_{j,expect} * \sigma_{detect,i} * \sigma_{detect,j} * \rho_{detect,ij}$

$$M_{detect} = \begin{bmatrix} 10*10*0.03*0.03*1 & 2*10*0.03*0.03*0 & 6*10*0.03*0.03*0 \\ 10*2*0.03*0.03*0 & 2*2*0.03*0.03*1 & 6*2*0.03*0.03*0 \\ 10*6*0.03*0.03*0 & 2*6*0.03*0.03*0 & 6*6*0.03*0.03*1 \end{bmatrix} = \begin{bmatrix} 0.09 & 0 & 0 \\ 0 & 0.0036 & 0 \\ 0 & 0 & 0.0324 \end{bmatrix}$$

These four statistical and systematic errors add to the final covariance matrix:

$$M = M_{stat} + M_{flux} + M_{cross} + M_{detect}$$

$$= \begin{bmatrix} 10 & 0 & 0 \\ 0 & 2 & 0 \\ 0 & 0 & 6 \end{bmatrix} + \begin{bmatrix} 2.25 & 0.225 & 0.675 \\ 0.225 & 0.09 & 0.135 \\ 0.675 & 0.135 & 0.81 \end{bmatrix} + \begin{bmatrix} 4 & 0.8 & 2.4 \\ 0.8 & 0.16 & 0.48 \\ 2.4 & 0.48 & 1.44 \end{bmatrix} + \begin{bmatrix} 0.09 & 0 & 0 \\ 0 & 0.0036 & 0 \\ 0 & 0 & 0.0324 \end{bmatrix}$$

$$= \begin{bmatrix} 16.34 & 1.025 & 3.075 \\ 1.025 & 2.2536 & 0.651 \\ 3.075 & 0.615 & 8.28240012 \end{bmatrix}$$

And the inverse covariance matrix is:

$$M^{-1} = \begin{bmatrix} 0.06706507 & -0.0241985 & -0.02310236 \\ -0.0241985 & 0.46164344 & -0.02529464 \\ -0.02310236 & -0.02529464 & 0.13119337 \end{bmatrix}$$

Then, once we've found the total inverse covariance matrix, we can calculate the χ^2 value for our observed data using Eq. 8, going through the summation one element at a time:

```
(Observe_1 - Expect_1)*M_{11}^{-1}*(Observe_1 - Expect_1) = (20-10)*0.06706507*(20-10) = 6.706507 (Observe_1 - Expect_1)*M_{12}^{-1}*(Observe_2 - Expect_2) = (20-10)*-0.0241985*(3-2) = -0.241985 (Observe_1 - Expect_1)*M_{13}^{-1}*(Observe_3 - Expect_3) = (20-10)*-0.02310236*(8-6) = -0.4620472 (Observe_2 - Expect_2)*M_{21}^{-1}*(Observe_1 - Expect_1) = (3-2)*-0.0241985*(20-10) = -0.241985 (Observe_2 - Expect_2)*M_{22}^{-1}*(Observe_2 - Expect_2) = (3-2)*0.46164344*(3-2) = 0.46164344 (Observe_2 - Expect_2)*M_{23}^{-1}*(Observe_3 - Expect_3) = (3-2)*-0.02529464*(8-6) = -0.05058928 (Observe_3 - Expect_3)*M_{31}^{-1}*(Observe_1 - Expect_1) = (8-6)*-0.02310236*(20-10) = -0.4620472 (Observe_3 - Expect_3)*M_{32}^{-1}*(Observe_2 - Expect_2) = (8-6)*-0.02529464*(3-2) = -0.05058928 (Observe_3 - Expect_3)*M_{32}^{-1}*(Observe_3 - Expect_3) = (8-6)*-0.02529464*(3-2) = -0.05058928 (Observe_3 - Expect_3)*M_{32}^{-1}*(Observe_3 - Expect_3) = (8-6)*-0.02529464*(3-2) = -0.05058928 (Observe_3 - Expect_3)*M_{32}^{-1}*(Observe_3 - Expect_3) = (8-6)*-0.02529464*(3-2) = -0.05058928 (Observe_3 - Expect_3)*M_{32}^{-1}*(Observe_3 - Expect_3) = (8-6)*-0.02529464*(3-2) = -0.05058928 (Observe_3 - Expect_3)*M_{32}^{-1}*(Observe_3 - Expect_3) = (8-6)*-0.02529464*(3-2) = -0.05058928
```

So, the final χ^2 sum is then:

$$\chi^2 = 6.706507 - 0.241985 - 0.4620472 - 0.241985 + 0.46164344 - 0.05058928 - 0.4620472 - 0.05058928 + 0.52477348 = 6.18368096$$

Applying χ^2 to Oscillations

Returning to the MicroBooNE MC data, we consider the "expected" data to be the intrinsic ν_e and ν_μ flux counts and compare this to the "observed" simulated oscillation signal flux (survival ν_e + appearance ν_e , as well as survival ν_μ). We do this because we want to compare all of the separate parameter oscillation signals to our "null" hypothesis of there being no oscillations, in order to determine which parameter combinations would create statistically significant oscillations.

I performed the chi^2 calculation over all of the ν_e and ν_μ spectra bins (including all ν_e and ν_μ appearance and disappearance channels) in order to give the χ^2 summation the most possible information, thus leading to a more accurate and sensitive chi^2 value.

For the 3+1 model which fits three parameters (Δm_{41}^2 , U_{e4} , and $U_{\mu 4}$) to the data, meaning a dof of 3, the χ^2 critical values are:

- $CL = 90\% \leftrightarrow \chi^2 = 6.251$
- $CL = 99\% \leftrightarrow \chi^2 = 11.345$
- $CL = 90\% \leftrightarrow \chi^2 = 16.266$

Any oscillation parameter combinations that produce a χ^2 less than the critical value would be considered outside of the sensitivity region because the experimental statistics can't confidently distinguish between the background neutrinos + noise and the oscillation signal.

Any oscillation parameter combinations that produce a χ^2 greater than the critical value would be considered within the sensitivity region, and if the true parameters exist within that region, the experiment will be able to detect that signal with statistical significance.

4 Results

4.1 χ^2 Contours in MicroBooNE Parameter Space

I calculated the oscillation probabilities and corresponding χ^2 values for 2,700 parameter combinations by stepping through the 3D parameter space created by Δm_{41}^2 , U_{e4}^2 , and $U_{\mu 4}^2$. Each axis contained 30 points spaced evenly on a log-10 scale with the limits:

- $0.1 < \Delta m_{41}^2 < 10$
- $0.0001 < U_{e4}^2 < 0.16$
- $0.0001 < U_{\mu 4}^2 < 0.16$

 $v_{\rm e}$ and v_{μ} Spectra χ^2 Sensitivity to Variations in $U_{\rm e4}^2$, $U_{\mu 4}^2$, and Δm_{41}^2 POT = 1.2e+21

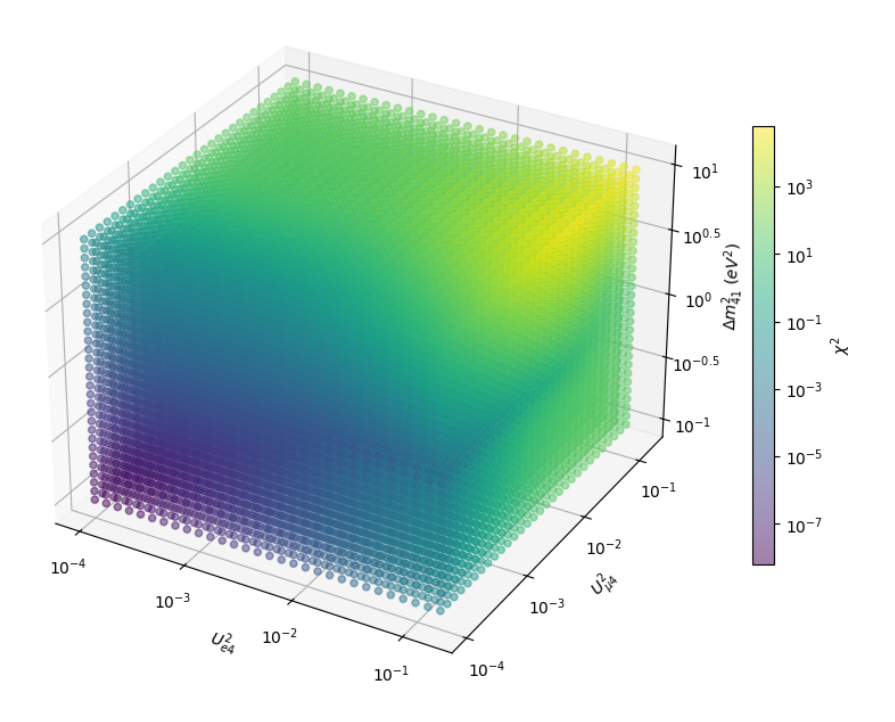


Figure 7: χ^2 values for each point within the 30x30x30 log-space grid in the Δm_{41}^2 , U_{e4}^2 , and $U_{\mu 4}^2$ parameter space

Plotting the corresponding χ^2 values as the colors in the 3D space gives Fig. 7 above. However, it is difficult to make out any contour details on this 3D plot, so I also looked at several 2D slices of the parameter space. Figure 8 below shows six slices in the Δm_{41}^2 vs U_{e4}^2 plane with varying $U_{\mu4}^2$ values and Figure 9 shows six slices in the perpendicular Δm_{41}^2 vs $U_{\mu4}^2$ plane with varying U_{e4}^2 values.

On these plots, the χ^2 critical values corresponding to the 90%, 99%, and 99.9% confidence levels are depicted as the white, red, and blue contour lines, and all of area to the

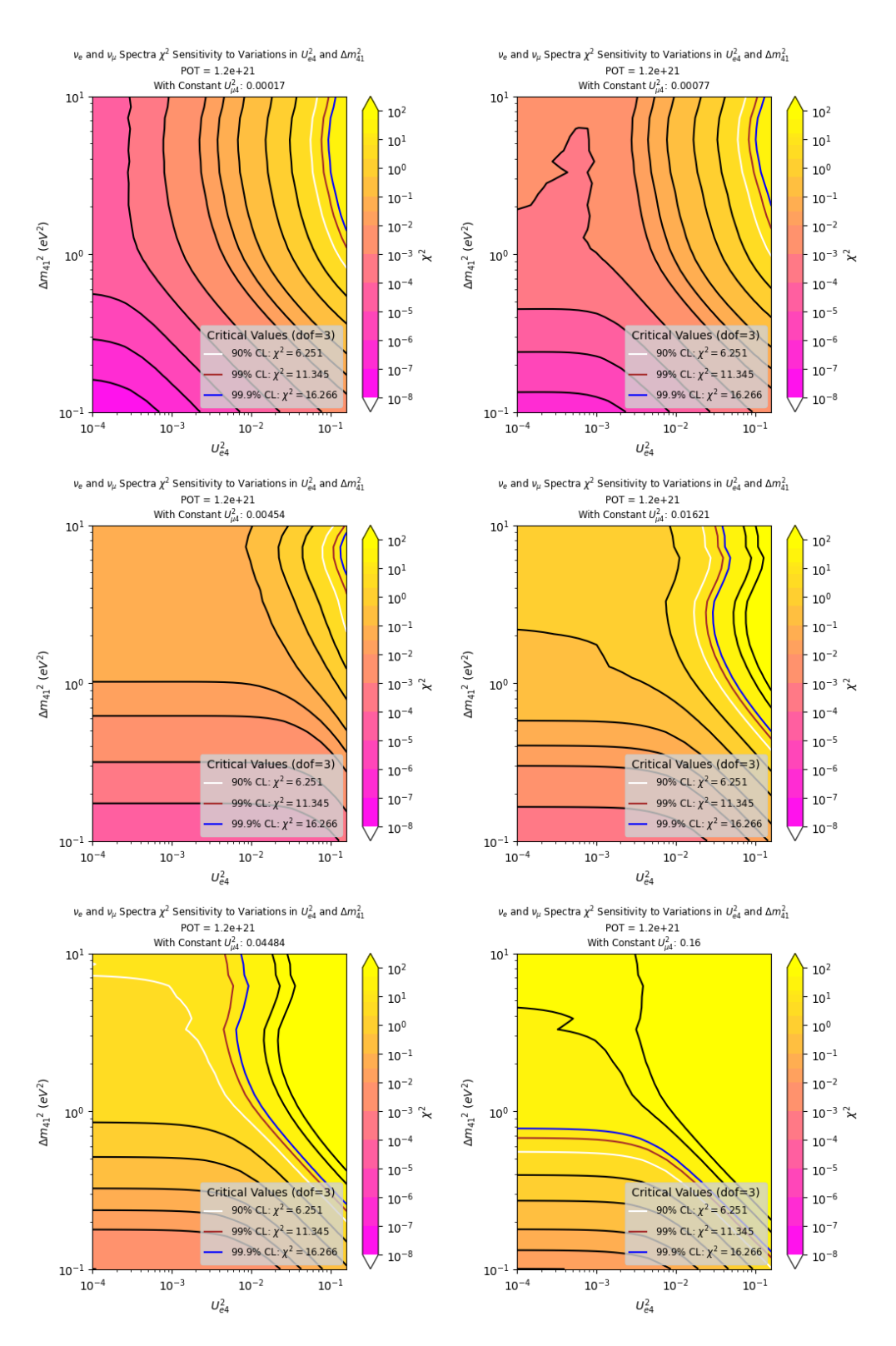


Figure 8: χ^2 color contours on 2D slices of the Δm^2_{41} vs U^2_{e4} plane with varying $U^2_{\mu4}$ values: 0.00017, 0.00077, 0.00454, 0.01621, 0.04484, 0.16 Animated GIF available at https://github.com/SarahPyth/Nevis_Labs_Neutrino_Reu_2024/blob/main/2D_chi2_contour_animation_deltam_Ue4.gif

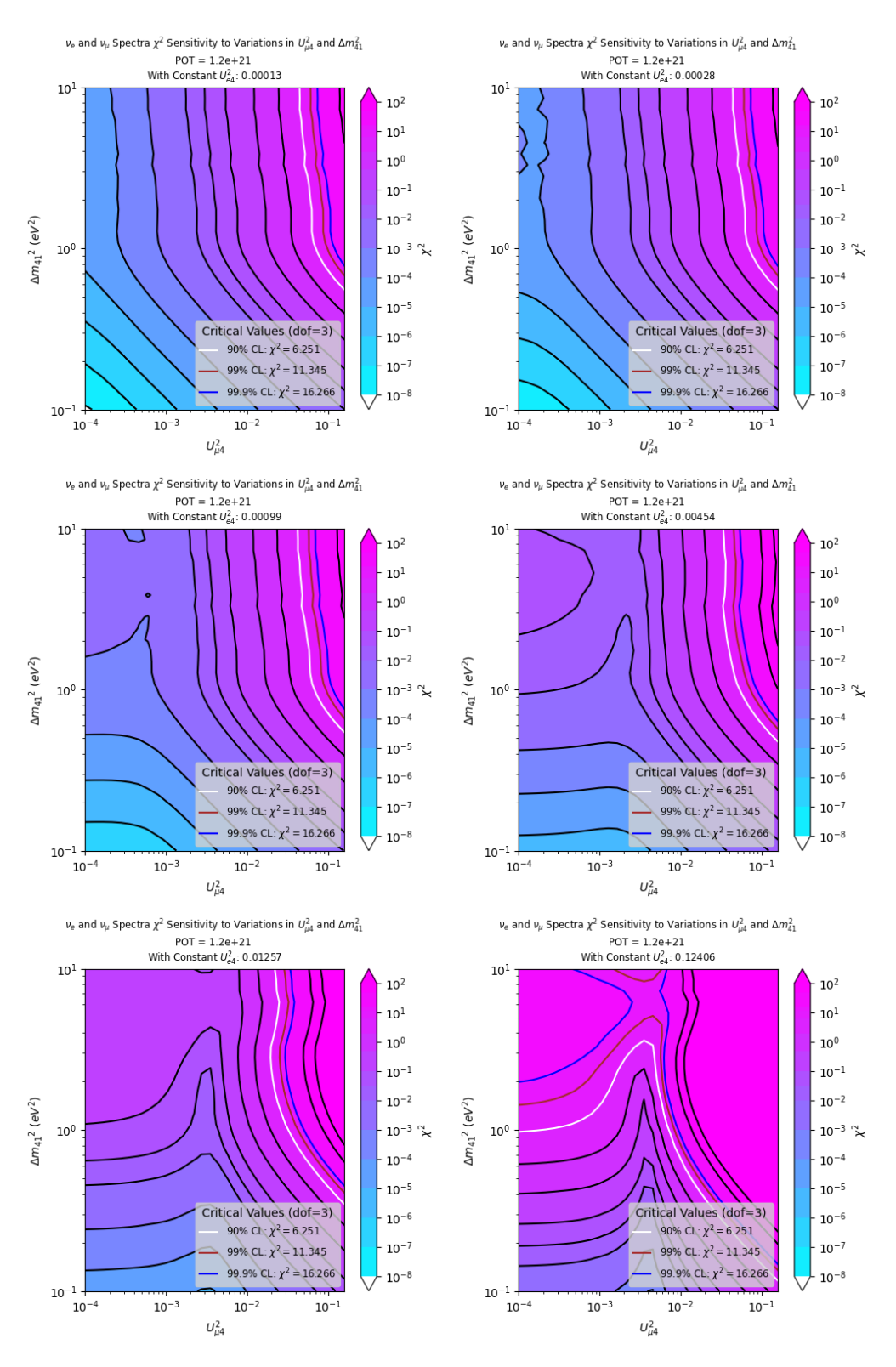
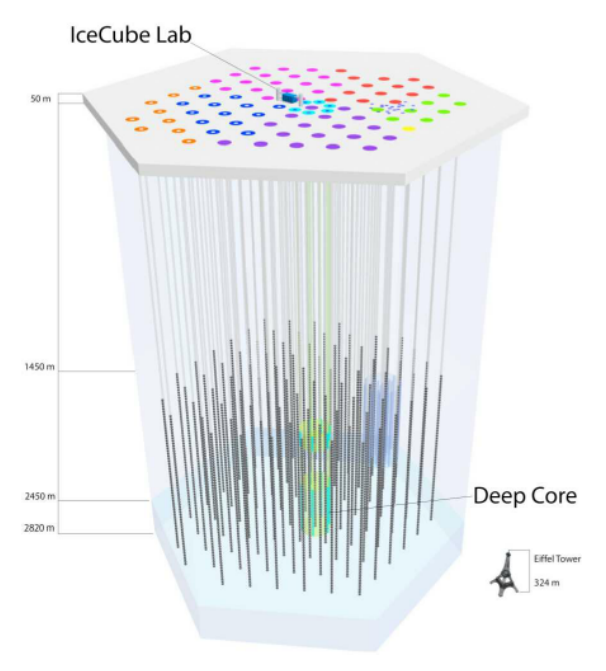


Figure 9: χ^2 color contours on 2D slices of the Δm^2_{41} vs $U^2_{\mu 4}$ plane with varying U^2_{e4} values: 0.00013, 0.00028, 0.00099, 0.00454, 0.01257, 0.12406 Animated GIF available at https://github.com/SarahPyth/Nevis_Labs_Neutrino_Reu_2024/blob/main/2D_chi2_contour_aimation_deltam_Um4. gif

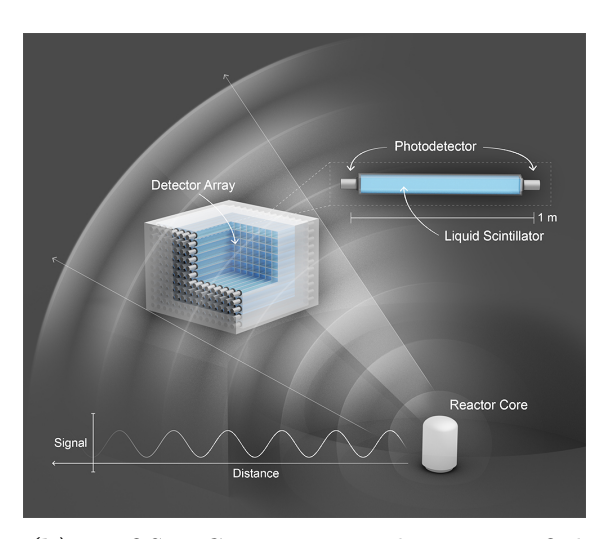
right of these contours has a χ^2 value above the critical values, indicating MicroBooNE has sensitivity to these parameter regions. All of the parameter regions to the left of the contours have χ^2 values less than the critical values, meaning MicroBooNE lacks sensitivity to these regions.

Additionally, on these χ^2 contour plots, we can see a χ^2 range from $10^{-8} < \chi^2 < 100$. We can also see that the χ^2 values have a spike of low values at approximately $U_{\mu 4}^2 \approx 0.006$ in Fig. 9. This can also be seen in Fig. 8 as the shrinking of the large χ^2 region in the upper right as $U_{\mu 4}^2$ increases, until a little after $U_{\mu 4}^2 = 0.00454$, when the region starts to rapidly grow again.

4.2 Incorporating External Constraints



(a) IceCube: Neutrino detector at South Pole that detects all neutrino flavors, but primarily measures atmospheric muon neutrino disappearance Image Credit: IceCube Collaboration



(b) PROSPECT: Neutrino detector at Oak Ridge National Labs that measures short baseline reactor electron antineutrino disappearance Image Credit: NIST/Sean Kelley

I also included external parameter information from two independent non-accelerator neutrino experiments: IceCube (Fig. 10a) and PROSPECT (Fig. 10b). IceCube's analysis found the best-fit parameters for the sterile neutrino model to be $\Delta m_{41}^2 = 4.5 eV$ and $sin^2(2\theta_{24}) = 0.1$ [10].

By specifying these two parameter values within the MicroBooNE oscillation probability equations and χ^2 calculation, I end up with a χ^2 plot that only depends on the single remaining free parameter $\sin^2(2\theta_{14})$, shown below in Figure 11.

Incorporating these IceCube best-fit constraints to the χ^2 analysis, MicroBooNE is only sensitive to the parameter region where $sin^2(2\theta_{14})$ is larger than ~ 0.25 (about 1/2 of the available parameter space).

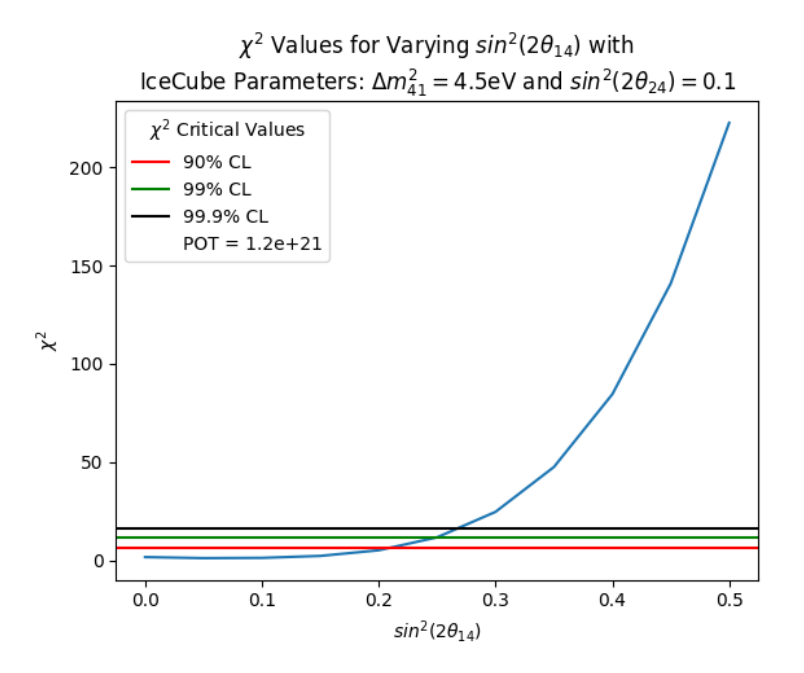


Figure 11: χ^2 values as a function of $\sin^2(2\theta_{14})$ holding $\Delta m_{41}^2 = 4.5 eV$ and $\sin^2(2\theta_{24}) = 0.1$ constant at the IceCube best-fit values

Then, I included the parameter constraining limits set by the PROSPECT experiment. PROSPECT's analysis found no evidence for sterile neutrino oscillations within its sensitivity parameter space, thus setting limits on the global parameter regions that could still contain 3+1 neutrino oscillations [11].

Looking at Fig. 12, if we choose to keep the IceCube best-fit value for Δm_{41}^2 at 4.5eV, we can see that PROSPECT rules out any $sin^2(2\theta_{14})$ greater than ~ 0.02 at a 99.73% confidence level [12].

Adding in this upper limit on $sin^2(2\theta_{14})$ on Fig. 13, we can see that only the $sin^2(2\theta_{14})$'s to the left of the vertical purple line are within this allowed region. We can clearly see that all of the $sin^2(2\theta_{14})$ values within this region lead to a χ^2 value below the critical values.

Thus, if we constrain the MicroBooNE 3+1 oscillation search by both IceCube's Δm_{41}^2 and $sin^2(2\theta_{24})$ best-fit values, as well as PROSPECT's $sin^2(2\theta_{14})$ upper limit, I find that MicroBooNE loses all sensitivity to this allowed parameter region.

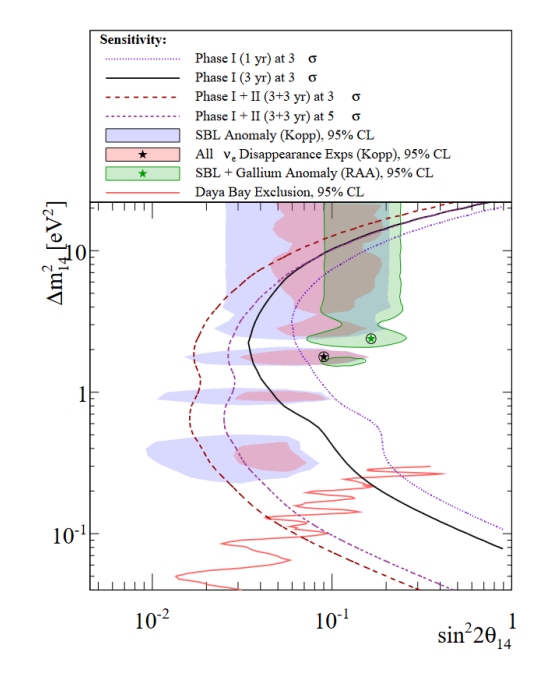


Figure 12: PROSPECT experiment's sensitivy curves in Δm_{41}^2 and $\sin^2(2\theta_{14})$ parameter space. Image Credit: PROSPECT Collaboration

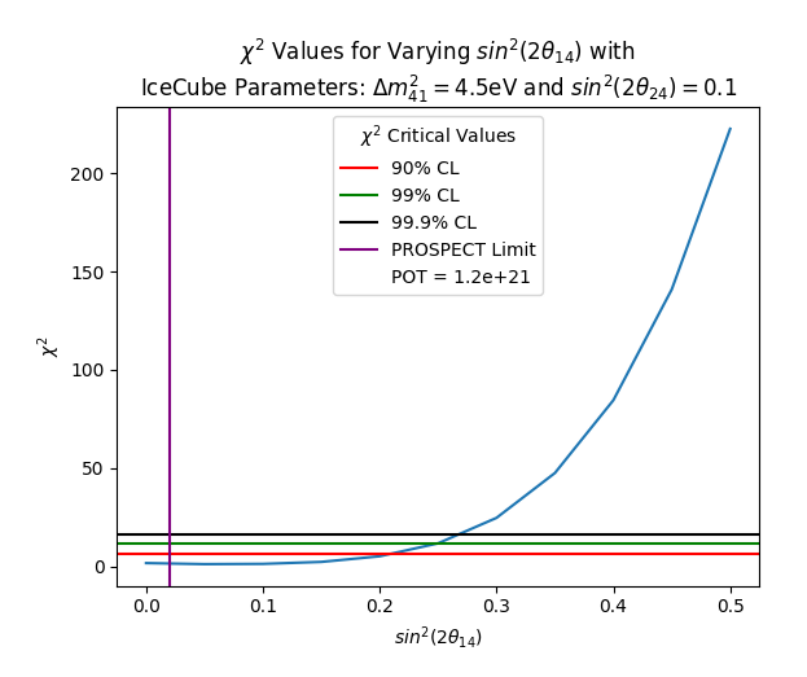


Figure 13: χ^2 values as a function of $\sin^2(2\theta_{14})$ holding $\Delta m_{41}^2 = 4.5 eV$ and $\sin^2(2\theta_{24}) = 0.1$ constant at the IceCube best-fit values with upper limit set by PROSPECT

5 Conclusion

In this study, I calculated the ν_e and ν_μ oscillation probabilities according to the 3+1 sterile neutrino model for the MicroBooNE experiment. I found the 3D parameter regions in Δm_{41}^2 , U_{e4}^2 , and $U_{\mu 4}^2$ for which MicroBooNE is sensitive at confidence levels of 90%, 99%, and 99.9%.

Additionally, I added in the external parameter constraints from both the IceCube and PROSPECT experiments, which found a best fit value for the Δm_{41}^2 and $sin^2(2\theta_{24})$ parameters, and an upper limit on the $sin^2(2\theta_{14})$ parameter respectively. Using both of these constraints, I found the MicroBooNE lost all sensitivity to the allowed parameter region.

This means that if both IceCube and PROSPECT's analysis is correct, MicroBooNE will not be sensitive enough to detect the true oscillation parameters, and thus will likely find no evidence for 3+1 neutrino oscillations within its own sensitivity parameter space. If, on the other hand, MicroBooNE does find strong evidence for 3+1 oscillations within its parameter space, this will directly oppose the results of IceCube and/or PROSPECT.

Acknowledgements

I'd like to thank my REU mentors Prof. Georgia Karagiorgi, Dr. Ibrahim Safa, and Prof. Mike Shaevitz. This material is based upon work supported by the National Science Foundation under Grant No. PHY-2349438.

References

- [1] P.A. Zyla et al. (Particle Data Group). "Review of Particle Physics Neutrino Masses, Mixing, and Oscillations". In: *Progress of Theoretical and Experimental Physics* 2020.8 (Aug. 2020), p. 083C01. ISSN: 2050-3911. DOI: 10.1093/ptep/ptaa104. eprint: https://doi.org/10.1093/ptep/ptaa104 (cit. on p. 3).
- [2] R. Acciarri et al. A Proposal for a Three Detector Short-Baseline Neutrino Oscillation Program in the Fermilab Booster Neutrino Beam. 2015. arXiv: 1503.01520 [physics.ins-det]. URL: https://arxiv.org/abs/1503.01520 (cit. on p. 5).
- [3] S Adrián-Martínez et al. "Letter of intent for KM3NeT 2.0". In: *Journal of Physics G: Nuclear and Particle Physics* 43.8 (June 2016), p. 084001. ISSN: 1361-6471. DOI: 10.1088/0954-3899/43/8/084001 (cit. on p. 6).
- [4] J. M. Conrad and M. H. Shaevitz. Sterile Neutrinos: An Introduction to Experiments. 2017. arXiv: 1609.07803 [hep-ex]. URL: https://arxiv.org/abs/1609.07803 (cit. on p. 7).
- [5] D. Cianci, A. Furmanski, G. Karagiorgi, and M. Ross-Lonergan. "Prospects of light sterile neutrino oscillation and CP violation searches at the Fermilab Short Baseline Neutrino Facility". In: *Physical Review D* 96.5 (Sept. 2017). ISSN: 2470-0029. DOI: 10.1103/physrevd.96.055001. URL: http://dx.doi.org/10.1103/PhysRevD.96.055001 (cit. on p. 9).
- [6] P. Abratenko et al. "First Constraints on Light Sterile Neutrino Oscillations from Combined Appearance and Disappearance Searches with the MicroBooNE Detector". In: *Physical Review Letters* 130.1 (Jan. 2023). ISSN: 1079-7114. DOI: 10.1103/physrevlett.130.011801. URL: http://dx.doi.org/10.1103/PhysRevLett.130.011801 (cit. on p. 11).
- [7] MicroBooNE Collaboration. Search for a Sterile Neutrino in a 3+1 Framework using Wire-Cell Inclusive Charged-Current e Selection with the BNB and NuMI beamlines in MicroBooNE. Public Note 1132. June 2024. URL: https://microboone.fnal.gov/wp-content/uploads/MICROBOONE-NOTE-1132-PUB.pdf (cit. on p. 11).
- [8] Carl Heiles. LEAST-SQUARES AND CHI-SQUARE FOR THE BUDDING AFI-CIONADO: ART AND PRACTICE. UC Berkeley Undergraduate Astronomy Lab, Mar. 2010. URL: http://ugastro.berkeley.edu/radio/2015/handout_links/lsfit_2008.pdf (cit. on p. 12).
- [9] MicroBooNE Collaboration. Search for a Sterile Neutrino in a 3+1 Framework using the Wire-Cell Inclusive Charged-Current e Selection from MicroBooNE. Public Note 1116. May 2022. URL: https://microboone.fnal.gov/wp-content/uploads/MICROBOONE-NOTE-1116-PUB.pdf (cit. on p. 12).

- [10] M. G. Aartsen et al. "eV-Scale Sterile Neutrino Search Using Eight Years of Atmospheric Muon Neutrino Data from the IceCube Neutrino Observatory". In: *Physical Review Letters* 125.14 (Sept. 2020). ISSN: 1079-7114. DOI: 10.1103/physrevlett. 125.141801. URL: http://dx.doi.org/10.1103/PhysRevLett.125.141801 (cit. on p. 19).
- [11] J. Ashenfelter et al. "First Search for Short-Baseline Neutrino Oscillations at HFIR with PROSPECT". In: *Physical Review Letters* 121.25 (Dec. 2018). ISSN: 1079-7114. DOI: 10.1103/physrevlett.121.251802. URL: http://dx.doi.org/10.1103/PhysRevLett.121.251802 (cit. on p. 20).
- [12] Karin Gilje. Sensitivity and Discovery Potential of the PROSPECT Experiment. 2015. arXiv: 1511.00177 [physics.ins-det]. URL: https://arxiv.org/abs/1511.00177 (cit. on p. 20).